

Synthesis of Ultrathin Silicon Nanosheets by Using Graphene Oxide as Template

Ziyang Lu,[†] Jixin Zhu,[†] Daohao Sim,[†] Wenwen Zhou,[†] Wenhui Shi,^{†,‡} Huey Hoon Hng,^{*,†} and Qingyu Yan^{*,†,§}[†]School of Materials Science and Engineering, Nanyang Technological University, 50 Nanyang Avenue, Singapore 639798, Singapore[§]TUM CREATE Centre for Electromobility, Singapore 637459[‡]ERIAN, Nanyang Technological University, Singapore 637553

Supporting Information

KEYWORDS: graphene oxide, Si nanosheets, Li ion battery

Two-dimensional (2D) nanostructures may show unique properties, as compared to zero- or one-dimensional ones because of their quantum well band structure and oriented surface exposure.¹ For example, graphene, which is basically a single layer of carbon atoms, attracted much interest because of its quantum hall effect,² high electrical/thermal conductivity,³ high mechanical strength,⁴ and high specific surface area.⁵ 2D structured topological insulators, such as HgTe or Bi₂Te₃, display massless Dirac-like surface states.⁶ And some catalysts, such as SiO₂,⁷ TiO₂,⁸ and Pd⁹ nanosheets, show good catalytic properties because of their high specific surface area.

Silicon is the most important material in modern electronic technology and its nanostructures show many promising potential applications due to size-confinement effect.¹⁰ Recently, the syntheses of silicon nanosheets have attracted great interest as they show many new properties.¹¹ For example, organosilicon nanosheets prepared by the reaction of polysilane with Grignard reagent have potential application in solar cells;^{11c} amine-modified Si nanosheets obtained by exfoliation of layered polysilane are easily self-assembled into a regular stacking structure.^{11e} However, these Si nanosheets are usually hybrid structures composed of Ca doping or methylamines and the size of these Si nanosheets are not controllable. Free standing single crystalline Si nanosheets can be synthesized by a chemical vapor deposition (CVD) process.^{11d} However, the diameter of the Si nanosheets cannot be controlled and this method may not be easily adapted for large scale production. As of now, it is still a challenge to develop scalable approaches to synthesize free-standing Si nanosheets with controllable size.

In this work, we report a controlled synthesis of ultrathin Si nanosheets with different sizes by using graphene oxide (GO) nanosheets as sacrificial templates. The GO sheets can be prepared abundantly by the oxidation and subsequent exfoliation of graphite.¹² The GO with different size ranges can be separated through the centrifuge process using different speeds. The synthesis of the Si nanosheets includes several steps (see the Supporting Information scheme S1). The GO sheets were first coated with a silica layer by a sol-gel process. The GO were then removed by calcining in air. The resulting silica sheets were then reduced to silicon by a thermal reduction

process assisted with magnesium powder. After acid etching, Si nanosheets were obtained. As an anode material, these Si nanosheets showed good Li storage properties.

Three types of GO sheets with different mean diameters of 400 nm, 4 and 10 μm were synthesized. Here, we chose the GO sheets with diameter of 4 μm to illustrate the whole synthesis process of the Si nanosheets. The GO sheets, which were prepared by a modified Hummer's method,¹³ contained many carboxyl, hydroxyl and epoxy groups as the nucleation sites for the growth of silica.¹⁴ The thickness of the GO sheets was determined from AFM measurements (see the Supporting Information, Figure S1a) to be ~ 0.9 nm, indicating that single layered GO sheets were obtained. After coating with a silica layer, the GO@SiO₂ retained the nanosheets structure as shown in the SEM image (Figure 1a). The thickness of the

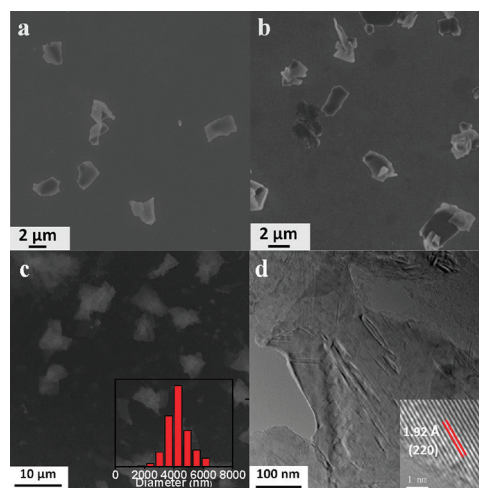


Figure 1. (a, b) SEM images of GO@SiO₂ nanosheets before and after calcination at 500 °C in air; (c, d) SEM and TEM images of Si nanosheets, Inset in c is a statistical size-distribution of 4 μm Si nanosheets; Inset in d is a high-resolution TEM image of a Si nanosheet.

Received: September 26, 2011

Revised: November 18, 2011

Published: November 22, 2011

GO@SiO₂ nanosheets was ~3.7 nm (see the Supporting Information, Figure S1b), which suggested that the thickness of the silica layer was about 1.4 nm on both sides of the GO sheets. Unfortunately, the TEM image (see the Supporting Information, Figure S2) did not show a clear contrast between the GO sheets and the SiO₂ layer. In order to prove that SiO₂ was successfully coated onto the GO sheets, we removed the GO sheets by calcining the samples at 500 °C in air. The corresponding TGA measurements (see the Supporting Information, Figure S3) confirmed that GO could be burned out at this temperature. After the calcination process, the remaining samples turned to white color and still retained the nanosheets structure (Figure 1b), which was expected to be SiO₂. Partial agglomeration of the nanosheets could be observed, but most of the nanosheets were not coarsened because the calcination temperature was not high enough to cause the nanosheets to cross-link.¹⁵ Furthermore, the peaks in the Raman spectra corresponding to the D-band (at 1350 cm⁻¹) and G-band (1588 cm⁻¹) of graphene oxides in the as-prepared GO@SiO₂ samples were not detectable after the calcination process (Supporting Information, Figure S4), which supports the removal of the GO in the calcined samples.

The SiO₂ nanosheets were reduced into silicon by mixing them with magnesium powder and annealing under Ar/H₂ atmosphere at 650 °C for 2 h, during which MgO was formed as a byproduct.¹⁶ The XRD patterns of the as-annealed samples (see the Supporting Information, Figure S5) showed the characteristic diffraction peaks of the cubic Si (JCPDF895012) as well as the cubic MgO (JCPDF790612). Unreacted SiO₂ was also expected to exist in the as-annealed samples. However, because of their amorphous nature, the unreacted SiO₂ was not detected from XRD analysis. MgO and the remaining SiO₂ were then removed by HCl and HF acid etching as described in the experimental section. Only peaks corresponding to the cubic Si phase were observed in the XRD patterns of the samples after the etching process, which indicated that MgO was removed. The energy-dispersive X-ray (EDX) analysis (Supporting Information Figure S6) showed that the intensity ratio between the (K) peaks of oxygen and Si decreased significantly (e.g., from 1 to 0.07) after the acid etching process, which suggested the removal of the oxides, e.g., SiO₂ and MgO.

After the etching process, the obtained Si maintained its nanosheets structure, which was revealed by the SEM and TEM images (Figure 1c, d). AFM measurement showed that the thickness of the Si nanosheets was ~3.5 nm, which was slightly thinner than that of the SiO₂ nanosheets (see the Supporting Information Figure S7). The HRTEM image (inset in Figure 1d) shows that these Si nanosheets were crystalline and the observed interlattice spacing of 0.192 nm corresponded to the (220) planes of cubic Si (JCPDF 895012). Unlike the SiO₂ nanosheets, defects such as pores could be observed in the Si nanosheets, which possibly formed during the acid etching process. Raman spectra of the Si nanosheets showed a peak at ~506 cm⁻¹, which was shifted from 520 cm⁻¹ of bulk silicon (see the Supporting Information, Figure S4). In addition, the full width at half-maximum (FWHM) of the peak was also widened to 30 cm⁻¹ as compared to bulk silicon (e.g., 20 cm⁻¹ for bulk silicon). Such Raman peak shift and broadening of the FWHM are attributed to the phonon confinement in the two-dimensional nanoscale Si crystal.¹⁷ The diameter of the Si nanosheets could be easily changed by using different sizes of GO as templates. Figure 2 shows the SEM images of Si nanosheets with mean diameter of 400 nm and 10 μm. It is

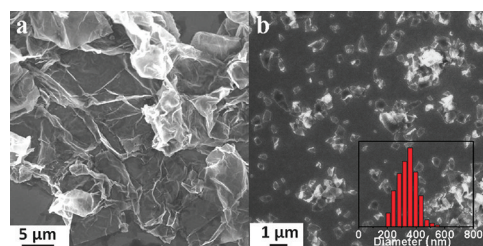
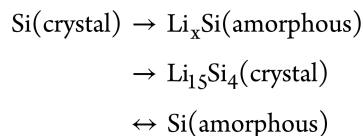


Figure 2. SEM images of (a) 10 μm and (b) 400 nm Si nanosheets. Inset in b is a statistical size-distribution of 400 nm Si nanosheets.

noted that the colloidal stability of the Si nanosheets decreased with increased diameters of the Si nanosheets. The 10 μm Si nanosheets are easily aggregated and it was hard to find individual Si nanosheets in the SEM images. On the contrary, Si nanosheets with diameter of ~400 nm could be easily dispersed into ethanol and remained separated as observed in the SEM image (Figure 2b). This was mainly due to the increased van der Waals attraction between the larger Si nanosheets.

A series of electrochemical measurements were carried out to study the Li storage properties of the Si nanosheets based on the half-cell configuration.¹⁸ The cyclic voltammetry (CV) curves of the first, second, and third cycles (see Figure S8 in the Supporting Information) were tested at a scan rate of 0.5 mV s⁻¹. The observed redox peaks in CV curves are in agreement with previous report and are related to the following conversion reactions¹⁹



The cycling performances of the Si nanosheets electrode were evaluated at 0.1 C (Figure 3). The Si nanosheet electrodes

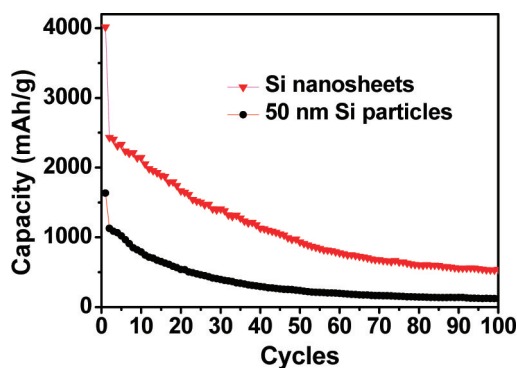


Figure 3. Cycling performance of different electrodes made of Si nanosheets and Si nanoparticles at a current density of 0.1 C.

maintained a discharge capacity of ~600 mA h g⁻¹ with a Coulombic efficiency of 96.2% during the 100th cycle. We also carried out similar tests on 50-nm silicon nanoparticles synthesized by direct reduction of SiO₂ using the same approach. The Si nanoparticles showed a lower initial discharge capacity of only 1636 mA h g⁻¹, which decreased rapidly to less than 120 mA h g⁻¹ during the 100th cycle. The higher initial capacities obtained in Si nanosheets as compared to that of Si nanoparticles is possibly due to its dimensional features. The ultrathin thickness (<5 nm) of the Si nanosheets allows the fast

kinetics of charge carrier diffusion as compared to that of the Si nanoparticles (~50 nm). The small feature size of the Si nanosheets may also effectively buffer the strain generated during the Li intercalation process. Furthermore, the large specific area of the Si nanosheets allows effective contact between the electrode and the electrolytes, which can also contribute to the high specific capacities.

In summary, we have developed a facile method to synthesize free-standing ultrathin silicon nanosheets by using GOs as sacrificial templates. The size of the Si nanosheets was controllable by using GO sheets of different sizes. The resulting Si nanosheets were well-crystallized, which showed better Li storage properties as compared to that of 50 nm Si nanoparticles. Such synthesis approaches can be promising for a scalable production of Si nanosheets.

■ ASSOCIATED CONTENT

■ Supporting Information

Experimental details, AFM images of GO, GO@SiO₂, TEM images of GO@SiO₂, XRD, EDX, and SEM analysis of the materials. This material is available free of charge via the Internet at <http://pubs.acs.org>.

■ AUTHOR INFORMATION

Corresponding Author

*E-mail: Alexyan@ntu.edu.sg and ashhhng@ntu.edu.sg.

■ ACKNOWLEDGMENTS

The authors gratefully acknowledge AcRF Tier 1 RG 31/08 of MOE (Singapore), NRF2009EWT-CERP001-026 (Singapore), Singapore Ministry of Education (MOE2010-T2-1-017), A*STAR SERC Grant 1021700144, and Singapore MPA 23/04.15.03 RDP 009/10/102 and MPA 23/04.15.03 RDP 020/10/113 grants.

■ REFERENCES

- (1) (a) Yoffe, A. D. *Adv. Phys.* **1993**, *42*, 173. (b) Tae, E. L.; Lee, K. E.; Jeong, J. S.; Yoon, K. B. *J. Am. Chem. Soc.* **2008**, *130*, 6534.
- (2) (a) Novoselov, K. S.; McCann, E.; Morozov, S. V.; Fal'ko, V. I.; Katsnelson, M. I.; Zeitler, U.; Jiang, D.; Schedin, F.; Geim, A. K. *Nat. Phys.* **2006**, *2*, 177. (b) Novoselov, K. S.; Jiang, Z.; Zhang, Y.; Morozov, S. V.; Stormer, H. L.; Zeitler, U.; Maan, J. C.; Boebinger, G. S.; Kim, P.; Geim, A. K. *Science* **2007**, *315*, 1379.
- (3) (a) Novoselov, K. S.; Geim, A. K.; Morozov, S. V.; Jiang, D.; Zhang, Y.; Dubonos, S. V.; Grigorieva, I. V.; Firsov, A. A. *Science* **2004**, *306*, 666. (b) Novoselov, K. S.; Geim, A. K.; Morozov, S. V.; Jiang, D.; Katsnelson, M. I.; Grigorieva, I. V.; Dubonos, S. V.; Firsov, A. A. *Nature* **2005**, *438*, 197. (c) Chen, J. H.; Jang, C.; Xiao, S. D.; Ishigami, M.; Fuhrer, M. S. *Nat. Nanotechnol.* **2008**, *3*, 206. (d) Balandin, A. A.; Ghosh, S.; Bao, W. Z.; Calizo, I.; Teweldebrhan, D.; Miao, F.; Lau, C. N. *Nano Lett.* **2008**, *8*, 902. (e) Xiao, N.; Dong, X. C.; Song, L.; Liu, D. Y.; Tay, Y.; Wu, S. X.; Li, L. J.; Zhao, Y.; Yu, T.; Zhang, H.; Huang, W.; Hng, H. H.; Ajayan, P. M.; Yan, Q. Y. *ACS Nano* **2011**, *5*, 2749.
- (4) Lee, C.; Wei, X. D.; Kysar, J. W.; Hone, J. *Science* **2008**, *321*, 385.
- (5) Stoller, M. D.; Park, S. J.; Zhu, Y. W.; An, J. H.; Ruoff, R. S. *Nano Lett.* **2008**, *8*, 3498.
- (6) (a) Bernevig, B. A.; Hughes, T. L.; Zhang, S. C. *Science* **2006**, *314*, 1757. (b) Qu, D. X.; Hor, Y. S.; Xiong, J.; Cava, R. J.; Ong, N. P. *Science* **2010**, *329*, 821.
- (7) Liu, J. H.; Wei, X. F.; Wang, X.; Liu, X. W. *Chem. Commun.* **2011**, *47*, 6135.
- (8) (a) Xiang, G. L.; Li, T. Y.; Zhuang, J.; Wang, X. *Chem. Commun.* **2010**, *46*, 6801. (b) Deng, Q. X.; Huang, C. Z.; Xie, W.; Zhang, J. P.; Zhao, Y. Q.; Hong, Z. S.; Pang, A. Y.; Wei, M. D. *Chem. Commun.*

2011, *47*, 6153. (c) Marani, D.; D'Epifanio, A.; Traversa, E.; Miyayama, M.; Licocchia, S. *Chem. Mater.* **2010**, *22*, 1126.

(9) (a) Huang, X. Q.; Tang, S. H.; Mu, X. L.; Dai, Y.; Chen, G. X.; Zhou, Z. Y.; Ruan, F. X.; Yang, Z. L.; Zheng, N. F. *Nat. Nanotechnol.* **2011**, *6*, 28. (b) Siril, P. F.; Ramos, L.; Beaunier, P.; Archirel, P.; Etcheberry, A.; Remita, H. *Chem. Mater.* **2009**, *21*, 5170.

(10) (a) Teo, B. K.; Sun, X. H. *Chem. Rev.* **2007**, *107*, 1454. (b) Sailor, M. J.; Wu, E. C. *Adv. Funct. Mater.* **2009**, *19*, 3195. (c) Wilcoxon, J. P.; Samara, G. A.; Provencio, P. N. *Phys. Rev. B* **1999**, *60*, 2704.

(11) (a) Nakano, H.; Mitsuoka, T.; Harada, M.; Horibuchi, K.; Nozaki, H.; Takahashi, N.; Nonaka, T.; Seno, Y.; Nakamura, H. *Angew. Chem., Int. Ed.* **2006**, *45*, 6303. (b) Morishita, T.; Russo, S. P.; Snook, I. K.; Spencer, M. J. S.; Nishio, K.; Mikami, M. *Phys. Rev. B* **2010**, *82*. (c) Sugiyama, Y.; Okamoto, H.; Mitsuoka, T.; Morikawa, T.; Nakanishi, K.; Ohta, T.; Nakano, H. *J. Am. Chem. Soc.* **2010**, *132*, 5946. (d) Kim, U.; Kim, I.; Park, Y.; Lee, K. Y.; Yim, S. Y.; Park, J. G.; Ahn, H. G.; Park, S. H.; Choi, H. J. *ACS Nano* **2011**, *5*, 2176. (e) Okamoto, H.; Kumai, Y.; Sugiyama, Y.; Mitsuoka, T.; Nakanishi, K.; Ohta, T.; Nozaki, H.; Yamaguchi, S.; Shirai, S.; Nakano, H. *J. Am. Chem. Soc.* **2010**, *132*, 2710.

(12) (a) Zhu, J. X.; Y, Z. Y.; Li, H.; Tan, H. T.; Chow, C. L.; Zhang, H.; Hng, H. H.; Ma, J.; Yan, Q. Y. *Small* **2011**, DOI: DOI:10.1002/smll.201101729. (b) Huang, X.; Yin, Z. Y.; Wu, S. X.; Qi, X. Y.; He, Q. Y.; Zhang, Q. C.; Yan, Q. Y.; Boey, F.; Zhang, H. *Small* **2011**, *7*, 1876.

(13) Xu, Y. X.; Bai, H.; Lu, G. W.; Li, C.; Shi, G. Q. *J. Am. Chem. Soc.* **2008**, *130*, 5856.

(14) Lee, K. G.; Wi, R.; Imran, M.; Park, T. J.; Lee, J.; Lee, S. Y.; Kim, D. H. *ACS Nano* **2010**, *4*, 3933.

(15) Yang, S. B.; Feng, X. L.; Wang, L.; Tang, K.; Maier, J.; Mullen, K. *Angew. Chem., Int. Ed.* **2010**, *49*, 4795.

(16) Bao, Z. H.; Weatherspoon, M. R.; Shian, S.; Cai, Y.; Graham, P. D.; Allan, S. M.; Ahmad, G.; Dickerson, M. B.; Church, B. C.; Kang, Z. T.; Abernathy, H. W.; Summers, C. J.; Liu, M. L.; Sandhage, K. H. *Nature* **2007**, *446*, 172.

(17) Faraci, G.; Gibilisco, S.; Pennisi, A. R.; Faraci, C. *J. Appl. Phys.* **2011**, *109*.

(18) Zhu, J. X.; Sun, T.; Chen, J. S.; Shi, W. H.; Zhang, X. J.; Lou, X. W.; Mhaisalkar, S.; Hng, H. H.; Boey, F.; Ma, J.; Yan, Q. Y. *Chem. Mater.* **2010**, *22*, 5333.

(19) (a) Hatchard, T. D.; Dahn, J. R. *J. Electrochem. Soc.* **2004**, *151*, A838. (b) Yu, Y.; Gu, L.; Zhu, C. B.; Tsukimoto, S.; van Aken, P. A.; Maier, J. *Adv. Mater.* **2010**, *22*, 2247. (c) Baranchugov, V.; Markevich, E.; Pollak, E.; Salitra, G.; Aurbach, D. *Electrochem. Commun.* **2007**, *9*, 796.